Supplemental Material

1. Determination of the diffusion and dispersion time constants of the NO and N_r measurements

The effect that diffusion and dispersion had on the effective time constants of the NO and N_r measurements was estimated from well understood transport and diffusion equations, and was determined experimentally from comparison of these measurements to the NO and NH_3 measurements made by the OP-FTIR at the sampling point at the top of the stack. The effects that sampling the atmosphere into a long tube has on the integrity of temporal information has been discussed by Karion et al., (2010). The figure of merit here is the root-mean square of the distance a gas molecule travels during the time the air sample transits from the stack to the instrument. This distance, X_{rms} can be calculated;

$$X_{rms} = (2Dt)^{1/2} \qquad \text{Eq S1.}$$

where D is the bimolecular diffusion coefficient of the analyte in air, and t is the time the diffusion is allowed to happen, in this case the 14 sec transit time from the stack to the instrument. Longitudinal mixing due to laminar flow, sometimes called dispersion, can add to the effective diffusion and can be estimated using the following relationship:

$$D_{eff} = D + a^2V^2/48D \qquad \text{Eq S2.}$$

where a is the inner radius of the tube, and V is the average flow velocity. Substituting the values of a and V, and using $D_{NO} = 0.23$ cm^2/sec (Tang et al., 2014), results in $X_{rms} \cong 40$cm. The linear velocity of the gas within the tube is 120 cm/sec, so based on simple diffusion and laminar flow dispersion, the effective time constant of the data acquired at 1 Hz would be degraded to about 2 second or so.

The comparison of the 1 Hz NO and N_r data with NO and NH_3 measurements acquired at the top of the stack by the OP-FTIR provides a useful means to check the effective time constant. Figure S1 shows the comparison of the chemiluminescence instrument measurements with the NO and NH_3 OP-FTIR measurements. The OP-FTIR had an effective sample acquisition/averaging time of 1.26 sec, so a 3-point smoothing of OP-FTIR signals results in an effective time constant of approximately 4 seconds.

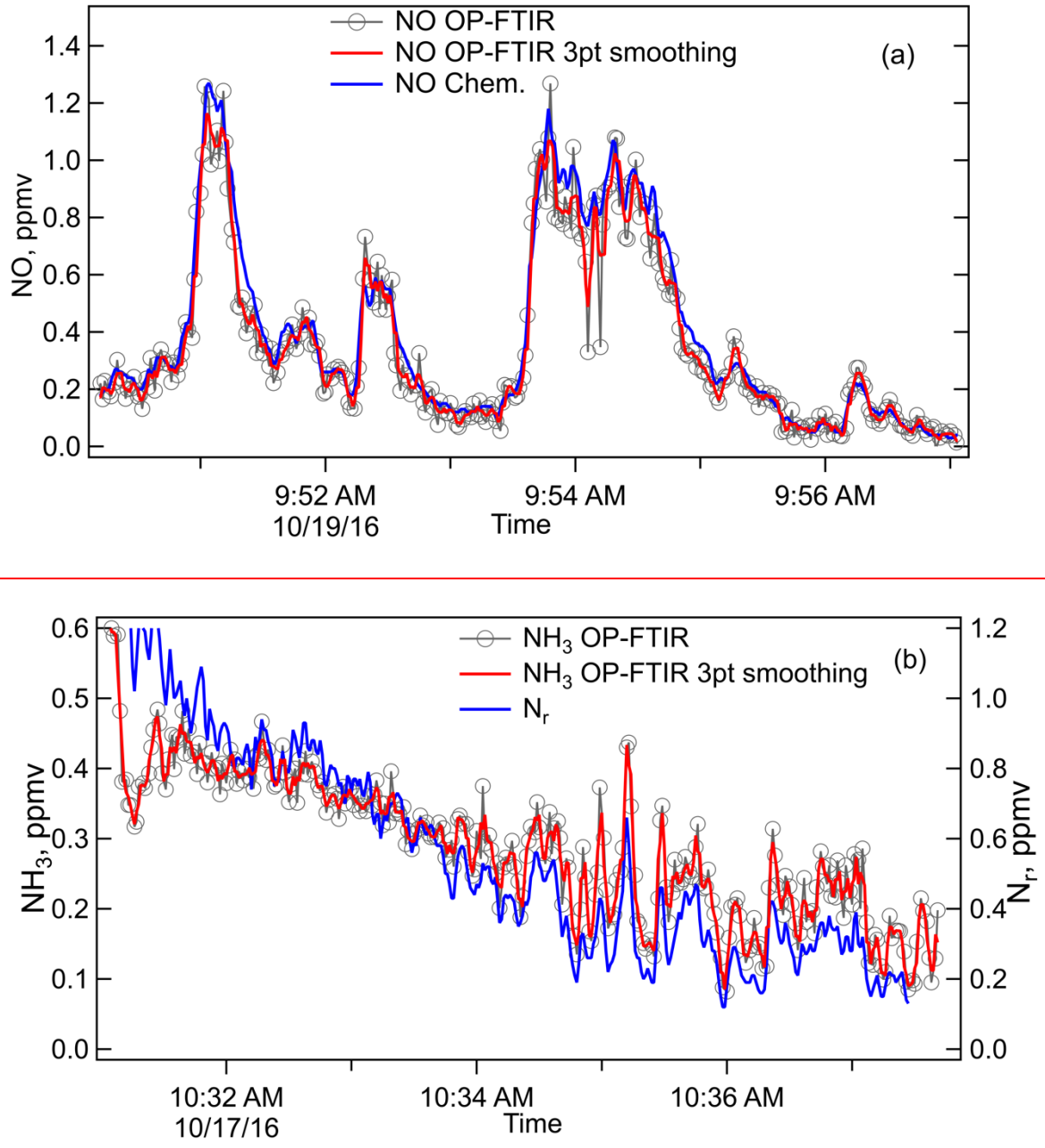

Figure S1. Comparison of the NO chemiluminescence measurement with that of the OP-FTIR (Panel a) for Fire 057, and comparison of the N_r measurement at the end of Fire 047 with the NH_3 measurement from the OP-FTIR (Panel b). Both the OP-FTIR 1.26 sec and the OP-FTIR data smoothed with a 3-pt box car method are shown.

2. Estimating the N lost to N_2 and N_2O.

The loss of N to N_2 and N_2O in the stack fires was estimated using the fuels data compiled in the Supplemental Material of Selimovic et al., [2018], and the ash data listed in

Table S1 of this Supplemental. The fuels data used in the analysis include: Total Fuel Mass, Total Residual Mass, %N Fuel (by weight), %C Fuel (by weight), and the ash data used in the analysis include: the ratio Ash/Burned Fuel, %N Ash (by weight), %Total C Ash (by weight). The gas phase measurements used for the analysis include: Total Reactive Nitrogen (N_r) reported here, and Total Carbon (CO_2 + CO + CH_4 +ΣNMOC + Particle Carbon), calculated in the manner described by Selimovic et al., [2018]. In the calculations below, we assume the Ash/Burned Fuel, %N Ash and %C Ash are the same for the stack burns as the quantities measured during the room burns. These assumptions add only a modest level of uncertainty since the fuels burned in each set of experiments were subsets of large samples of each fuel type, and the use of Ash/burned fuel removes some of the variability in fire conditions and extent, as it accounts for unburned residual fuel. Another source of uncertainty is the application of fuel moisture measurements. In general, the correction for fuel moisture applies equally to foliage (needles) and woody biomass, but there are occasions where those were not equal or the residual fuel was more heavily represented by woody biomass. Residual masses were often 10% of the initial fuel mass, but sometimes as high as 50% of initial mass. Considering these factors, we estimate an uncertainty in the mass balance calculations to be ±25%.

The mass balance equations for Nitrogen and Carbon are;

Mass N emitted = Mass Total Fuel *%N Fuel – Mass Ash*%N Ash – Mass Unburnt residual *%N Fuel = Mass (N_r + N_2 + N_2O) Eq. S3

Where: Mass Unburnt residual = Mass Total Residual – Mass Ash Eq. S4.

and

Mass C emitted = Mass Total Fuel *%C Fuel – Mass Ash*%C Ash – Mass Unburnt residual *%C Fuel = Mass (CO_2 + CO +CH_4 +NMOC + Particle C) = Mass Total C Eq. S5

Where: Mass Unburnt residual = Mass Total Residual – Mass Ash Eq. S6.

There are measured concentrations of N_r, and Total C, however there were not accurate measurements of the actual flow rates of air up the stack. The concentrations (mixing ratios) of N and C species are related to mass flow by several constants, e.g. pressure, temperature, Avogadro's number, all of which are the same for both N and C, except for the atom weights. As a consequence, we can use the ratios of concentrations to obtain the following relationships;

$$\frac{(N_r+N_2+N_2O)}{\text{Total C}} = \frac{(\text{Mass Total Fuel *\%N Fuel – Mass Ash*\%N Ash – Mass Unburnt residual *\%N Fuel})/14g}{(\text{Mass Total Fuel *\%C Fuel – Mass Ash*\%C Ash – Mass Unburnt residual *\%C Fuel})/12g} \quad \text{Eq. S7}$$

Recognizing that;

$$\frac{(N_2+N_2O)}{\text{Total C}} = \frac{(\text{Mass Total Fuel *\%N Fuel – Mass Ash*\%N Ash – Mass Unburnt residual *\%N Fuel})/14g}{(\text{Mass Total Fuel *\%C Fuel – Mass Ash*\%C Ash – Mass Unburnt residual *\%C Fuel})/12g} - \frac{N_r}{\text{Total C}} \quad \text{Eq. S8}$$

The ratio of Eqs. S8 and S7 gives;

(N_2+N_2O) /$(N_r+N_2+N_2O)$ = The fraction of N lost as N_2 and N_2O, estimated from fuel and ash composition and the measured quantity N_r/Total Carbon.

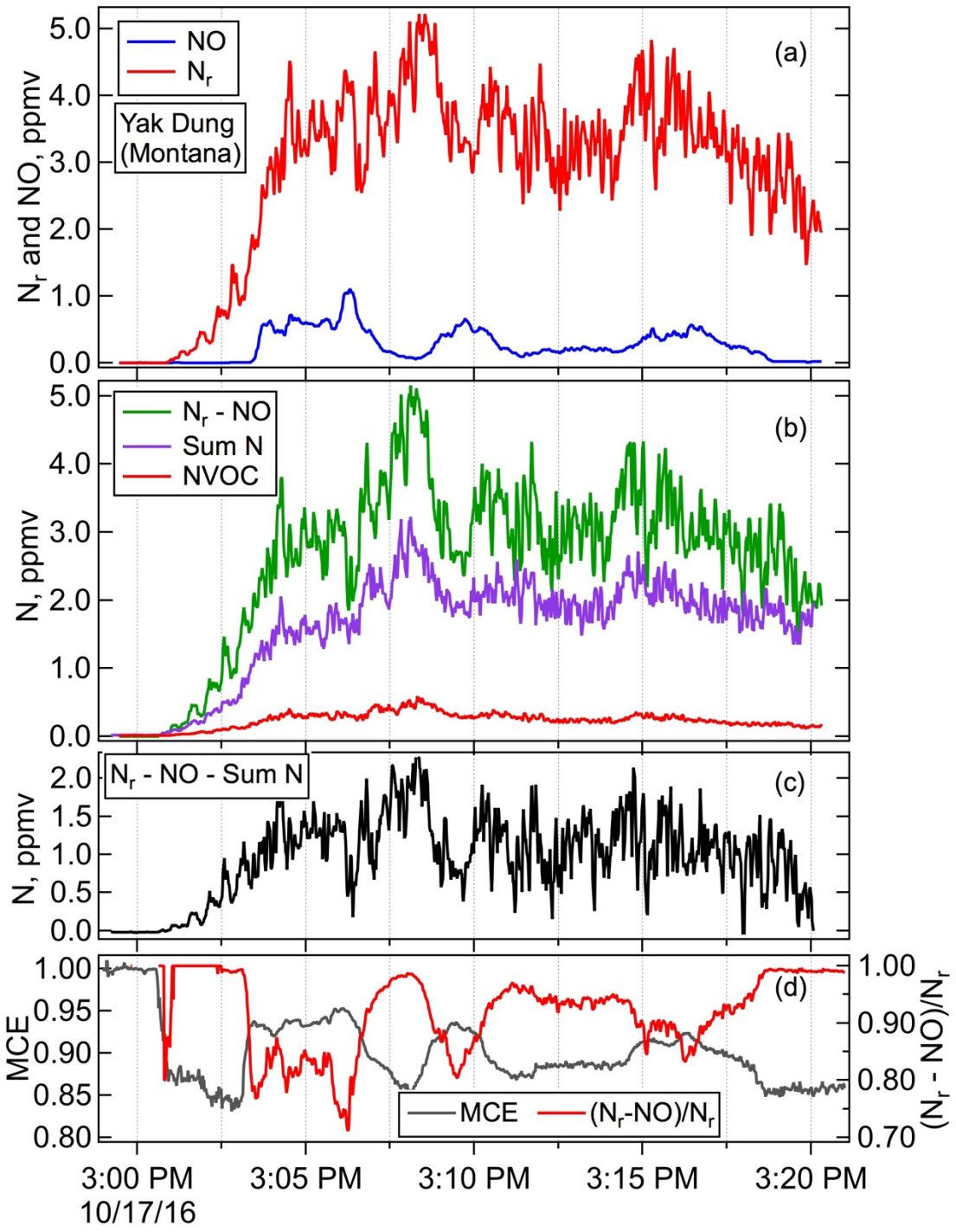

Figure S2. Timelines of N_r and NO (panel a), N_r-NO, the sum of all measured N_r species except for NO (panel b), and residual of N_r minus all measured N species (N_r-NO-Sum N, panel c) and MCE and $(N_r-NO)/N_r$ (panel d) for Fire050, Montana yak dung.

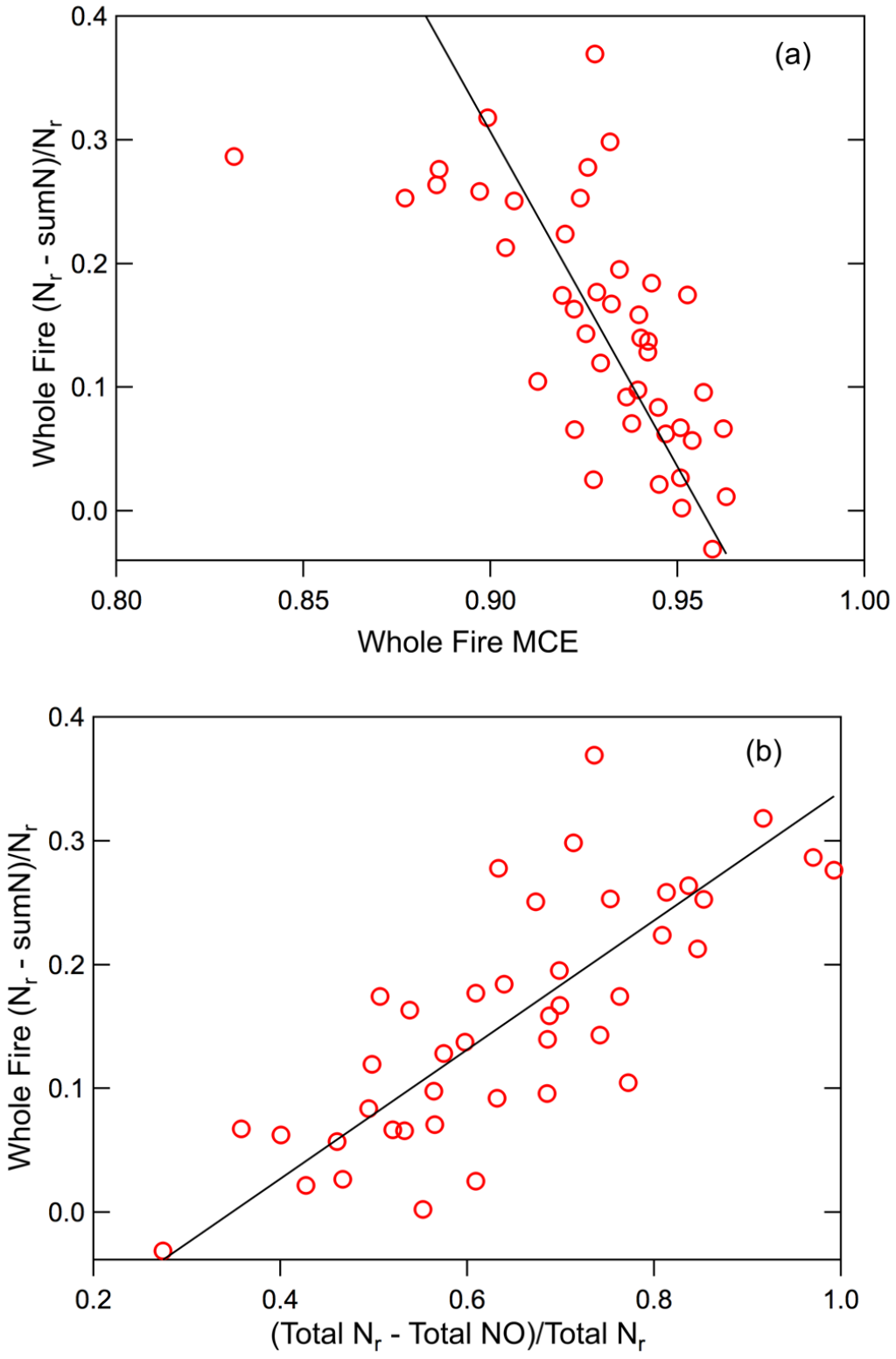

Figure S3. The relative amounts of residual N_r vs MCE (a) and vs (N_r-sumN)/N_r (b) for whole fires. The lines are orthogonal-distance-regression fits that assume uncertainty in each variable.

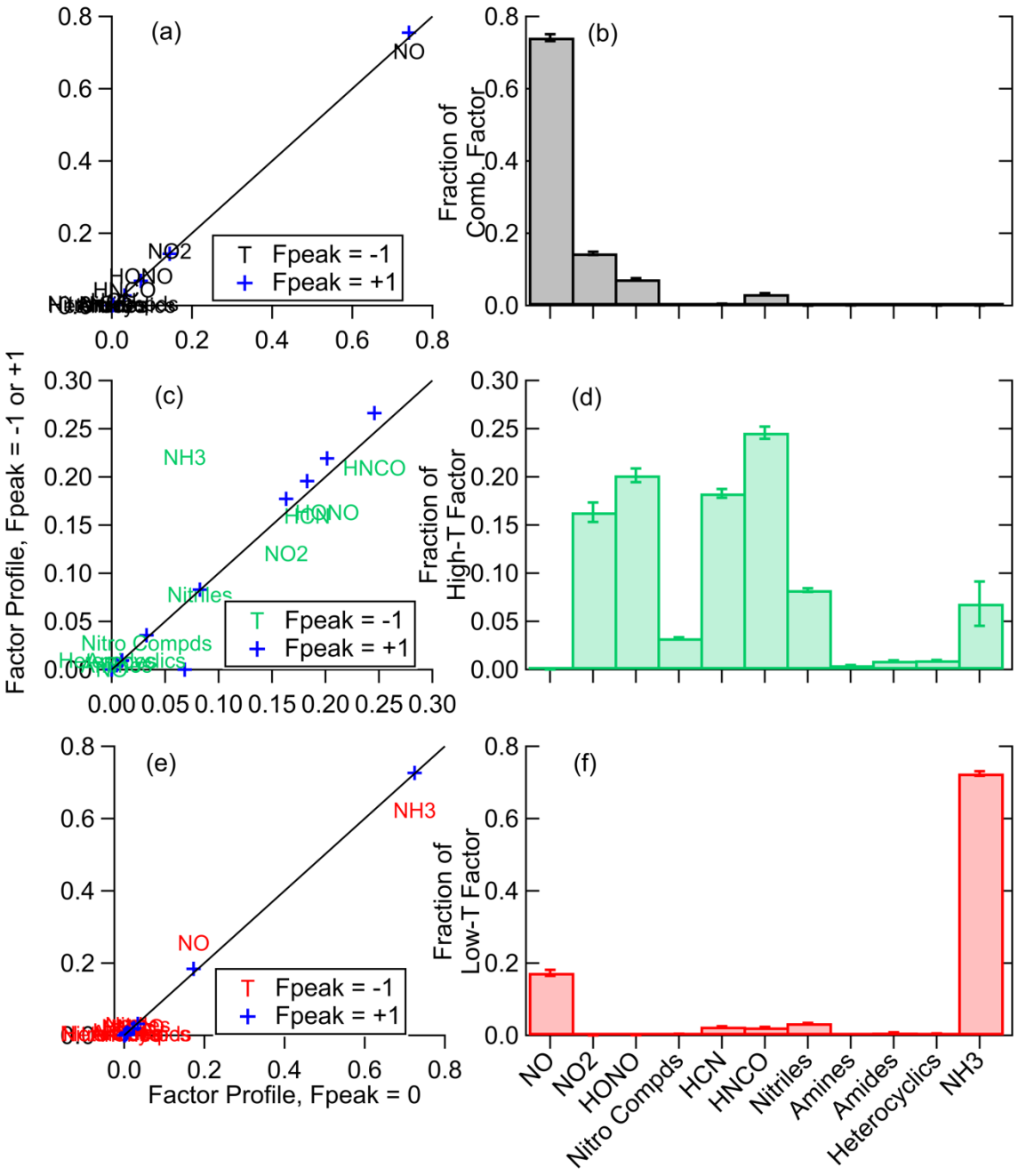

Figure S4. Details of the PMF analysis of Fire 063. Figures S4 a, c and e show that the Fpeak=0 solution is stable compared to Fpeak -1 and +1. Figures b, d, and f show that the three factor solution is robust with respect to different initial factor profiles (seeds) for 100 different runs.

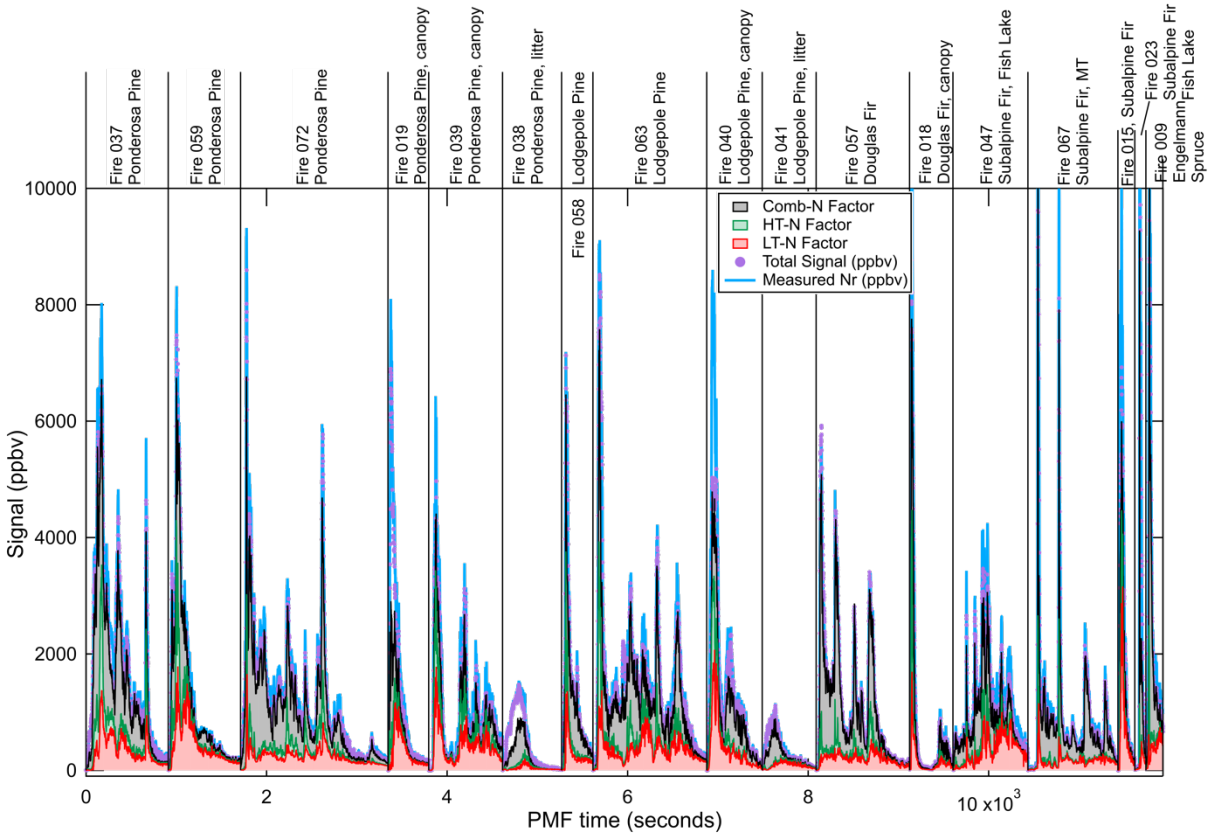

Figure S5. Combined PMF timeline for the fires that involved coniferous fuels. The measured N_r is shown as a blue line, the total of N_r compounds used in the PMF is shown as purple points, and Comb-N (grey), HT-N (green), and LT-N (red) factors plotted stacked on top of one another. The vertical lines show where individual fires start and stop.

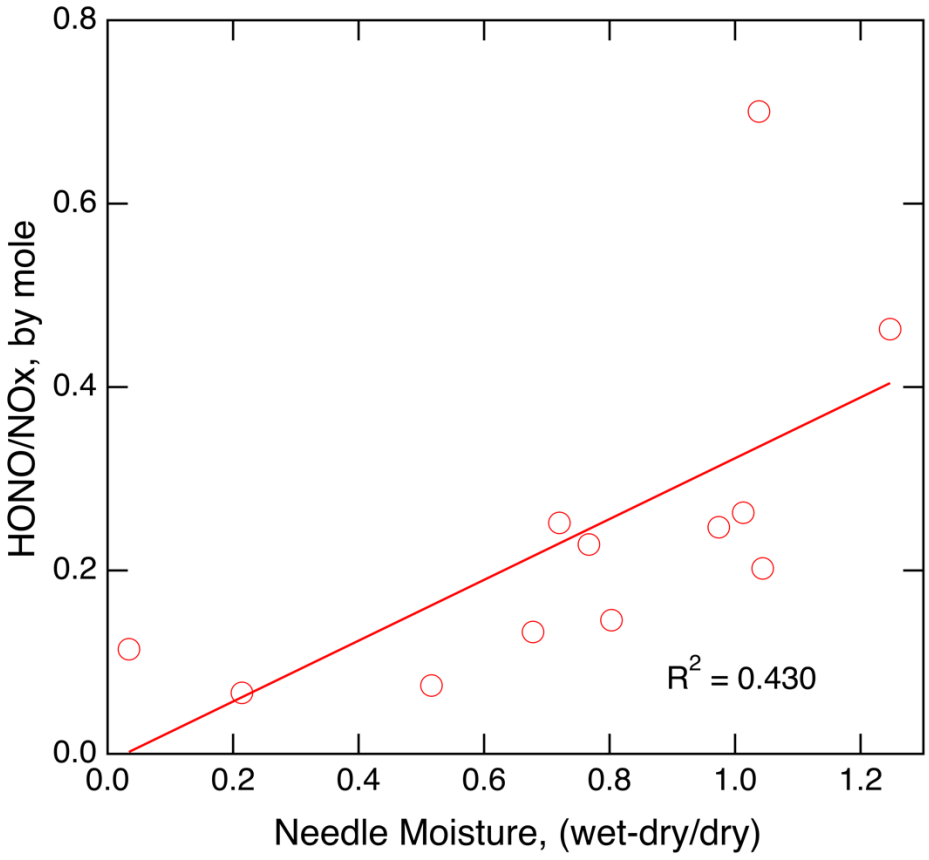

Figure S6. The correlation of HONO/NOx (by mole) with needle moisture for fires that were canopy fuels only (Fires 015, 017, 018, 019, 020, 023, 025, 039, 040, 044, 045, and 064).

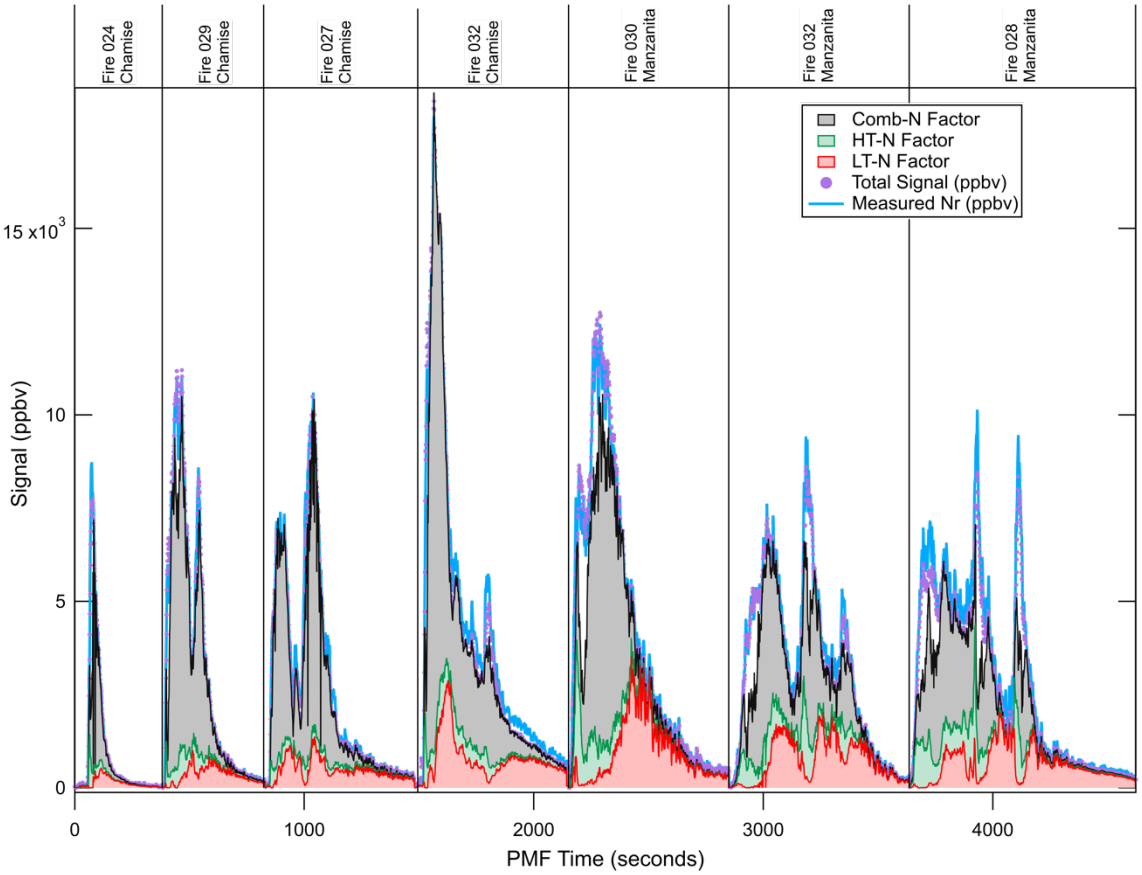

Figure S7. The timeline for the combined PMF analysis of chaparral fuels. The measured N_r is shown as a blue line, the total of N compounds used in the PMF is shown as purple points, and Comb-N (grey), HT-N (green), and LT-N (red) factors plotted stacked on top of one another. The vertical lines show where individual fires start and stop.

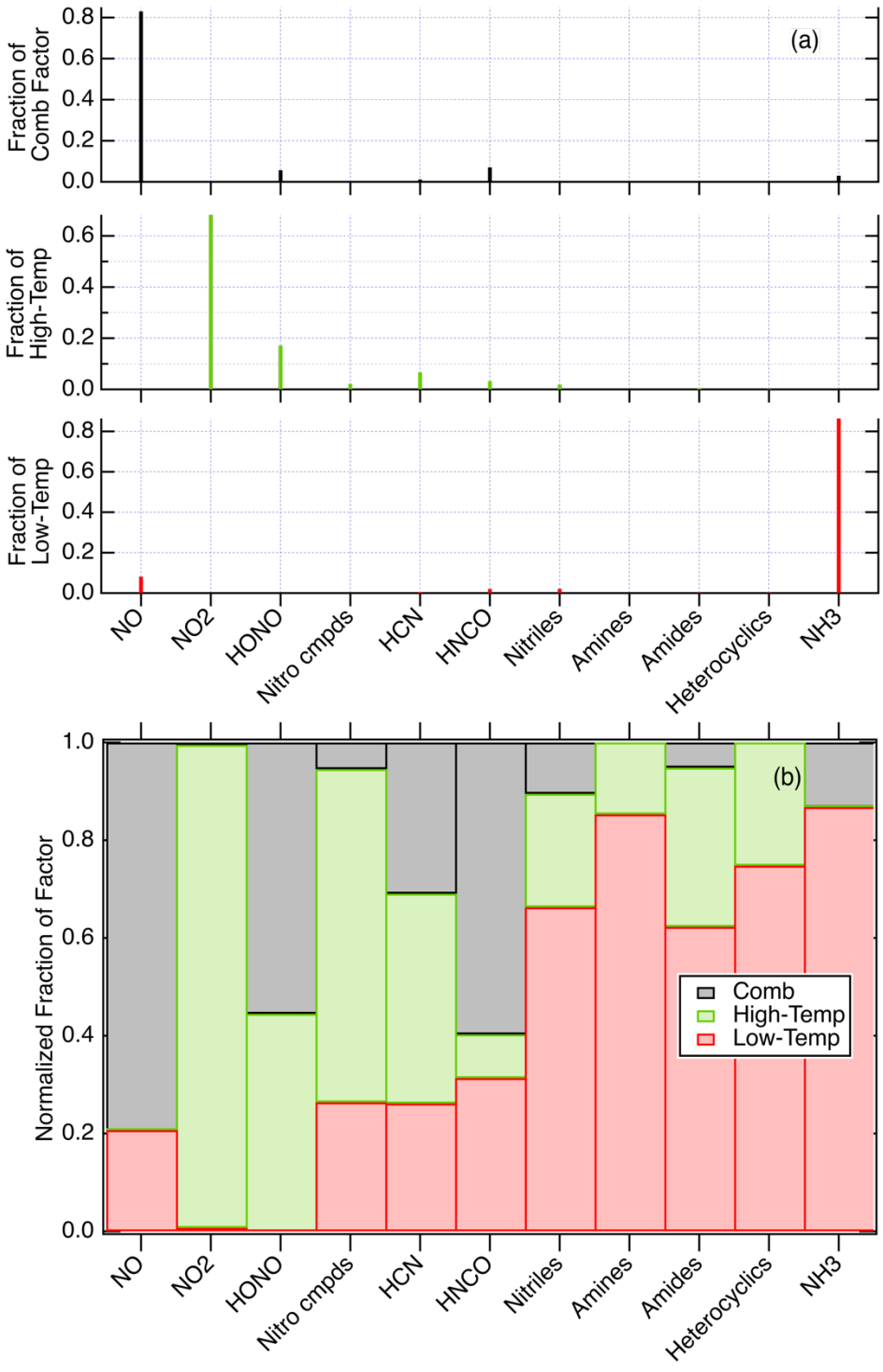

Figure S8. The contributions of nitrogen species to the factors that simulate the emissions from chaparral fuels shown in Figure S7 (panel a), and the fraction of each compound or class found in each factor (panel b).

References:

Karion, A., Sweeney, C., Tans, P., and Newberger, T.: AirCore: An innovative atmospheric sampling system, J. Atmos. Ocean. Technol., 27, 1839-1853, 2010.

Tang, M. J., Cox, R. A., and Kalberer, M.: Compilation and evaluation of gas phase diffusion coefficients of reactive trace gases in the atmosphere: volume 1. Inorganic compounds, Atmos. Chem. Phys., 14, 9233-9247, 2014.